k-Space

2

Michael Loecher and Oliver Wieben

Abstract

This chapter will introduce the k-space formalism used in MR imaging for data encoding and image reconstruction via Fourier transforms (FT). Essentially, this formalism is a mathematical construct that allows for the description of acquired MRI data in a domain described as spatial-frequency space, or k-space, which is related to the desired image space representation via the Fourier transform. Representing the data as k-space converts the time varying signal acquired with the MR receiving coils into a 2D or 3D data space that can be readily reconstructed into an image representation by applying the well-known Fourier transform. Understanding MRI acquisitions and reconstructions in terms of k-space is a crucial step in understanding the basic relationships between the acquisition and the reconstructed images, most acceleration and reconstruction techniques, sources of artifacts and their appearance, and advanced acquisition strategies.

Keywords

k-space formalism • Fourier transform • Spatial resolution • Field-of-view • Sampling • Receiver bandwidth • Spatial frequency • Sampling trajectory

This chapter will review the principles of data acquisitions in frequency space along with the implications that the choice of acquisition parameters, such as sampling frequency and receiver bandwidth, have on the resulting image parameters such as spatial resolution, field-of-view (FOV), spatial aliasing, and others. The k-space formalism also allows for a convenient and intuitive interpretation of sampling patterns, usually referred to as k-space trajectories, through the use of pulsed magnetic field gradients. This concept will be discussed along with standard rectilinear or Cartesian sampling and examples of echo-planar MRI as well as radial and spiral trajectories. For a more extensive derivation of these concepts and the underlying mathematics, the interested reader is referred to textbooks [1–3].

M. Loecher, PhD
Department of Medical Physics, University of Wisconsin-Madison, 1111 Highland Ave, Suite 1127, Madison, WI 53705-2275, USA

O. Wieben, PhD (✉)
Department of Medical Physics, University of Wisconsin-Madison, 1111 Highland Ave, Suite 1127, Madison, WI 53705-2275, USA

Department of Radiology, University of Wisconsin-Madison, 1111 Highland Ave, Suite 1127, Madison, WI 53705-2275, USA
e-mail: owieben@wisc.edu

Introduction to k-Space

The ultimate goal in MR imaging is the generation of a diagnostically useful image that represents the spatial distribution of certain tissue properties as influenced by the spin distribution, relaxation parameters, and physiological factors such as flow, motion, and diffusion. Some early MRI approaches exploited pointwise scanning of the object [4]. This method is very time-consuming and extremely

M.A. Syed et al. (eds.), *Basic Principles of Cardiovascular MRI: Physics and Imaging Technique*,
DOI 10.1007/978-3-319-22141-0_2

limited in its signal-to-noise ratio (SNR) because of the inherently low signal that arises from a single voxel. This approach somewhat resembles the use of a digital camera that has only a single sensor to acquire signal from each individual voxel one after another in a sequential digitization process, instead of the actual simultaneous use of many light receptors.

Instead, MR data acquisition is conducted in a transform domain called *Fourier space*, which is also called *frequency space*. In MRI, this domain is commonly referred to as *k-space* based on nomenclature established by physicists and mathematicians to describe spatial frequencies in equations that contain propagating waves such as light, sound, or radio waves [5]. This terminology precedes its use in MR imaging, and the letter '*k*' is neither an abbreviation nor does it have a specific meaning.

Acquiring data in an alternative domain is not necessarily intuitive at a first glance, but can offer many advantages. This approach is not uncommon in medical imaging; consider, for example, the use of the Radon transform for Computed Tomography (CT) image reconstruction from projection data. One tremendous advantage of k-space acquisition is that the net magnetization in every voxel of the imaging volume contributes to the received signal simultaneously, thereby greatly amplifying the SNR and scan efficiency. While many transforms share this property, MR data acquisition is conducted in Fourier space because the time-varying gradient waveforms used for imaging give rise to a signal equation that directly resembles the Fourier transform (FT) and therefore ensures a straightforward image reconstruction using 2D or 3D FT as shown in Fig. 2.1. This is somewhat of a fortunate coincidence for the field of MRI and the realization of the k-space formalism [6–8] has greatly advanced the field.

Signal Equation and k-Space

We can represent an extremely simplified MRI signal equation as:

$$S(t) = \iiint I(\boldsymbol{r}) e^{i\gamma \boldsymbol{r} \cdot \int_0^t \boldsymbol{G}(t')dt'} d^3r \tag{2.1}$$

Where $S(t)$ is the free-induction decay (FID) or echo detected by an RF receiver coil; $I(\boldsymbol{r})$ describes the signal associated with spatial location or point $\mathbf{r}$, which is dependent on several factors including proton density, T_1 and T_2 relaxation, as well as imaging parameters; i is the imaginary unit; γ is the nuclear gyromagnetic ratio; and $\boldsymbol{G}(t)$ is a vector quantity that represents the magnetic field gradient at time t after the magnetic excitation. We can then substitute:

$$\boldsymbol{k}(t) = \gamma \int_0^t \boldsymbol{G}(t')dt' \tag{2.2}$$

to simplify Eq. 2.1 and we obtain:

$$S(t) = \iiint I(\mathrm{r}) e^{i\mathbf{k}(t)\cdot \mathrm{r}} d^3r \tag{2.3}$$

where we can see the relationship between the acquired signal, $S(t)$, the original object, $I(\boldsymbol{r})$, and the spatial-frequency distribution, $\boldsymbol{k}(t)$.

In this notation, the signal equation which links the data acquired with the RF receiver coil to the spatial distribution of the underlying MR signal sources resembles the Fourier transform. Mapping the acquired FID to its corresponding value of $k(t)\cdot r$ gives us our k-space representation, where the acquired time varying data is mapped onto a spatial frequency coordinate system relating it to the applied gradients. In this context, the k-space representation can be either two

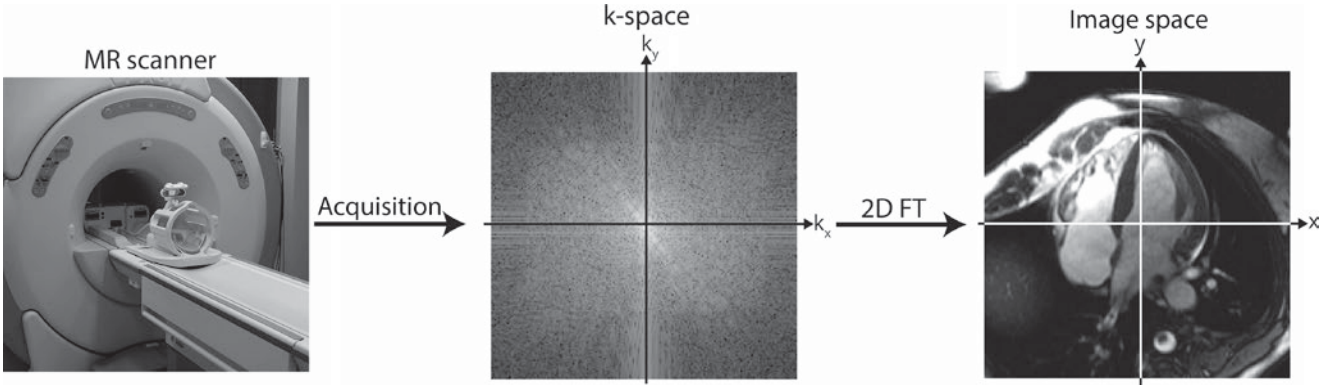

Fig. 2.1 The acquisition and reconstruction process for MR imaging. Data is collected using RF receiver coils. Through the use of time varying gradients, the data are acquired in Fourier space, also commonly referred to as k-space. A Fourier transform (FT) is required to reconstruct the desired image that displays the signal distribution in spatial coordinates

or three dimensional, depending on the acquisition scheme. In general, $\boldsymbol{k}(t)$ has three directional components, commonly notated as *kx*, *ky*, and *kz*. The acquired k-space data points are complex valued and correspond to spatial frequencies with units of 1/distance.

Spatial Frequencies

The acquisition of the weighting coefficients of spatial frequencies is central to MR imaging as it is based on the concept that any image can be represented in Fourier space as a weighted sum of harmonic functions of multiple spatial frequencies and orientations. Thereby, the data representation in image space and frequency space are linked with the Fourier transform [3].

This relationship is illustrated in Fig. 2.2, where the underlying patterns of three representative spatial harmonics are explored in more detail. Datapoint (O) represents the weighting coefficient for a low spatial frequency in the *ky-direction* and the zero spatial frequency in the *kx*-direction. The spatial frequency is inversely proportional to the wavelength. Consequently, it represents a wave pattern of moderately long wavelength, λ_O, which is strictly oriented along the y-axis. Datapoint (P) has components in *kx* and *ky* and represents a diagonal wave pattern, here of higher spatial frequency with a shorter wavelength, λ_P. Datapoint (Q) is a special case as it represents the origin of the coordinate system, which corresponds to the sum of the signal in the image across all voxels, thereby reflecting the average signal intensity of the image when properly scaled. The resulting image is composed of the sum of all wave patterns weighted by the coefficient (grayscale value) in the k-space representation. It can be shown that any image can be accurately decomposed into the sum of these weighted wave patterns with varying wavelengths and angle orientations. The weighting coefficients of the wave patterns are displayed in grayscale as the k-space representation of the image.

Data Properties in Image Space and k-Space

In MRI, the k-space data, also referred to as the raw MR data, are directly measured and the corresponding image space is reconstructed by performing an inverse 2D or 3D Fourier transform. It is noteworthy that the process is reciprocal: for a known image, forward FT can generate the corresponding k-space representation, a fact that can be important for example in certain iterative reconstructions. It is further important to note that the Fourier transform generally generates complex valued data in both domains. In MR imaging, the acquired k-space signal is complex valued as it is obtained with quadrature coils containing a real and an imaginary channel. The MR image is also complex valued due to various factors including magnetic susceptibility, chemical shift, data inconsistencies from motion and flow artifacts, acquisition imperfections such as eddy currents and gradient delays, and other factors that cause the image to deviate from what would ideally be real-valued.

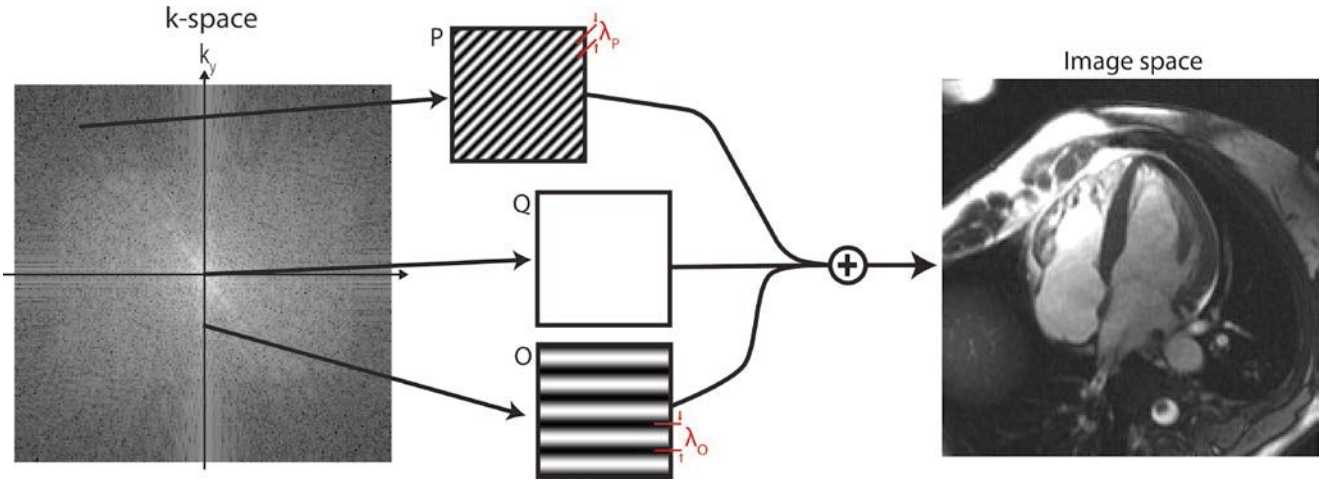

Fig. 2.2 A visual interpretation of the use of spatial harmonics to decompose an image. Every individual point in k-space represents a spatial frequency that can be represented as a wave of a certain frequency and corresponding wavelength, λ, as well as direction of the wave pattern. The image can be formed by the summation of all wave patterns weighted by their k-space coefficient, which is represented as a grayscale value in the k-space map. Representative pictures of the spatial harmonics are shown for select points O, P, and Q, with their corresponding wavelengths, λ_O and λ_P

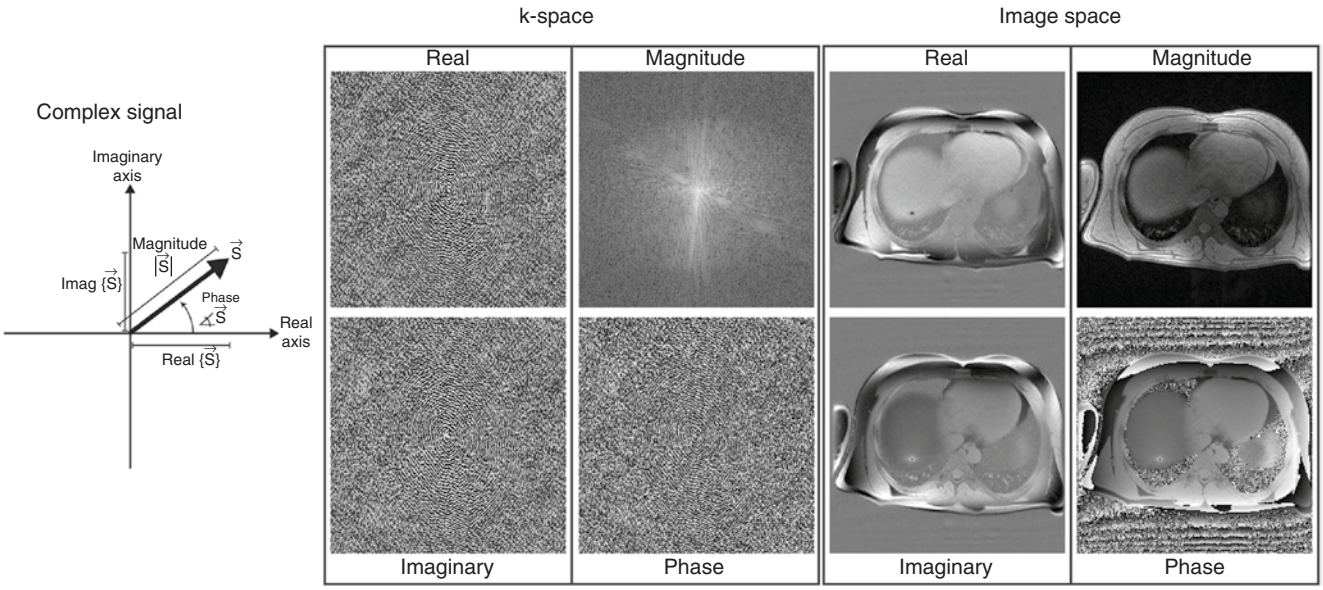

Fig. 2.3 All data from an MR system with quadrature RF coils are complex valued and can be described either by their magnitude and phase or by their real and imaginary components. Often, the image display and storage is reduced to the magnitude display. The in vivo head scan shows that an MR image is not real valued as there are phase contributions from system imperfections and effects such as magnetic susceptibility, motion, and flow

Consequently, a complete data representation in k-space or in image space requires the display of either the real and imaginary channel, or an equivalent display of magnitude and phase of the complex valued signal as shown in Fig. 2.3. The reconstruction process always generates a complex valued image data set. However, in most clinical scans the phase image is discarded and only the magnitude image is utilized for diagnosis. There are some exceptions where diagnostic information is contained in the phase data, including phase contrast MRI, MR elastography, susceptibility weighted imaging, spectroscopy, and fat-water imaging approaches. These techniques require the processing of the phase data in image space in addition to the magnitude data. Alternatively, the data can be stored as a real and an imaginary channel from which magnitude and phase can be derived as shown in Fig. 2.3.

As described above, the center spatial frequency, also called the DC component because it reflects a non-varying image component similar to a direct current, represents the sum of the signal in all voxels in image space. Consequently, it is a very high signal, usually orders of magnitude higher than almost all other k-space coefficients. It is typical in MR images for most of the signal energy to be concentrated in the lower spatial frequencies because the imaging scene is dominated by large, high contrast objects. Therefore, the k-space data are commonly displayed with a logarithmic grayscale as shown in Fig. 2.4. Otherwise, the dynamic range of the display is not sufficient to distinguish signal variances in the lower signal regions, i.e., the outer regions of k-space. The k-space data are usually displayed in the form of a magnitude representation since there is little added value to the human observer to display the k-space phase, or to display the real and imaginary channels. The most essential information, namely the distribution of energy in k-space, is contained in the magnitude component. Nonetheless, it is essential for the reconstruction engine to use complex-valued k-space data and not the magnitude alone.

Matrix Sizes and Artifacts

When using the Fourier transform, the matrix sizes in both domains are identical. In a 2D case, MxN k-space data points are mapped onto MxN image space data points. However, this one-to-one mapping does not always hold true as we introduce acceleration techniques, which allow us to reconstruct more image pixels from less acquired data under certain assumptions, as will be explored in greater detail in Chap. 5. It is important to note that this one-to-one mapping does not mean that a specific data point in k-space reconstructs to a specific data point in image space. In fact, each single point in k-space will influence *all* of the pixels in image space, because each value in k space represents a harmonic function over the whole image. This concept is essential in understanding and identifying some of the artifacts found in MRI, such as those described in Fig. 2.5.

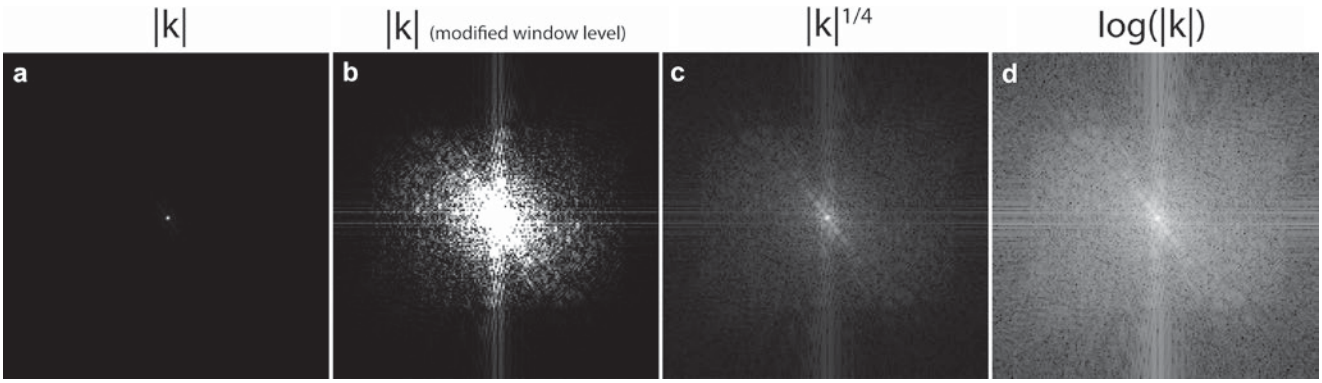

Fig. 2.4 k-space magnitude displays of the cardiac scan shown in Fig. 2.2 with various scaling schemes. As the center of k-space can be on the order of 10,000 times greater than the edges of k-space, a non-linear display of the grayscale can be advantageous. (**a**) k-space values linearly mapped to greyscale values and using the full dynamic range of the acquired data, which suppressed any signal outside the very center of k space. (**b**) Same as (**a**), except window and level settings have been changed to cap off higher signals to better appreciate lower values. (**c**, **d**) Data scaling with an exponential or logarithm scale can improve the visualization of the smaller values as seen in the higher spatial frequency components

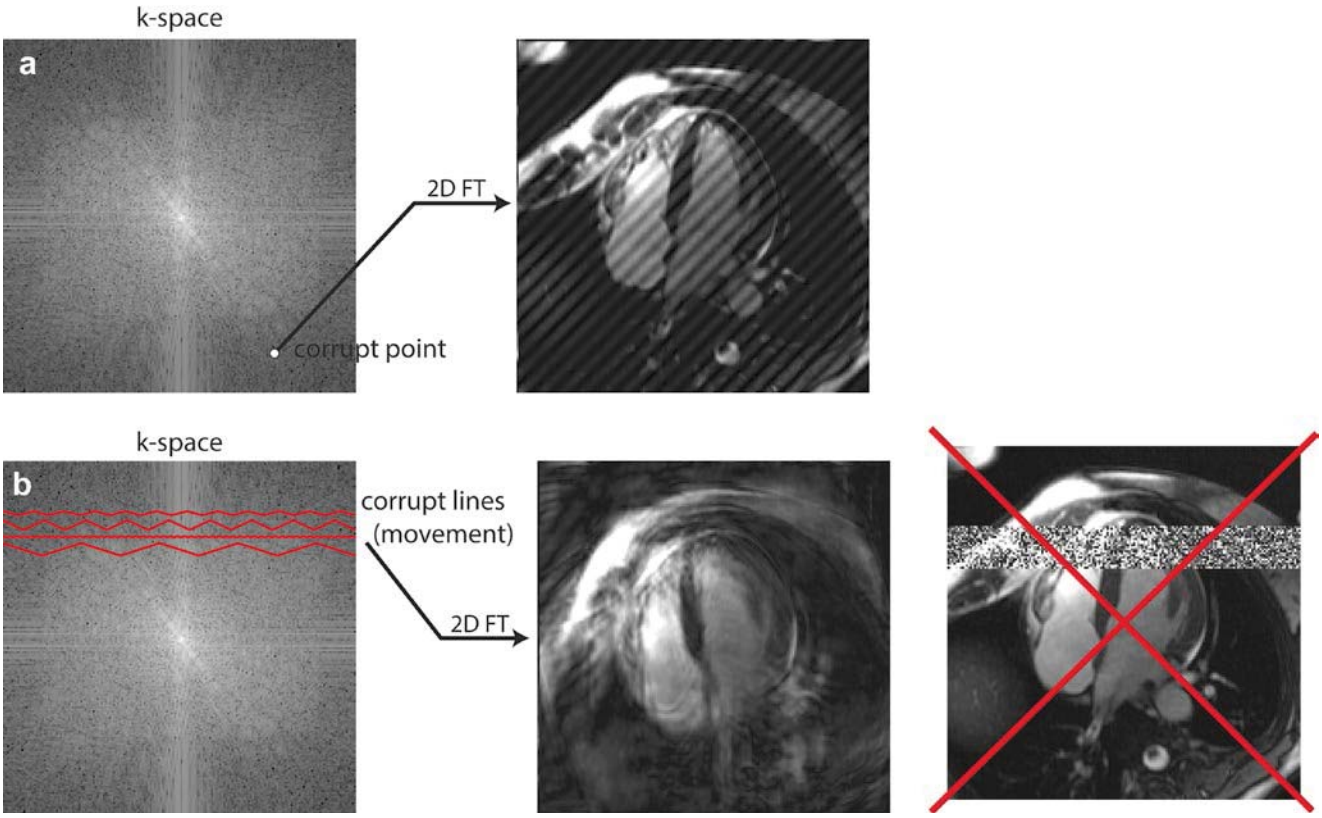

Fig. 2.5 Errors in k-space manifest in image space based on the spatial frequencies affected. (**a**) If a single point in k-space is corrupt, that particular spatial frequency will appear enhanced or reduced in the reconstructed image as shown in this "corduroy" or "spiking" artifact. (**b**) If a patient moves during an acquisition, those portions of k-space will be corrupt and can lead to decreased image quality. These errors will be reflected in the whole image and not only in a single region of the image as shown here for illustration purposes

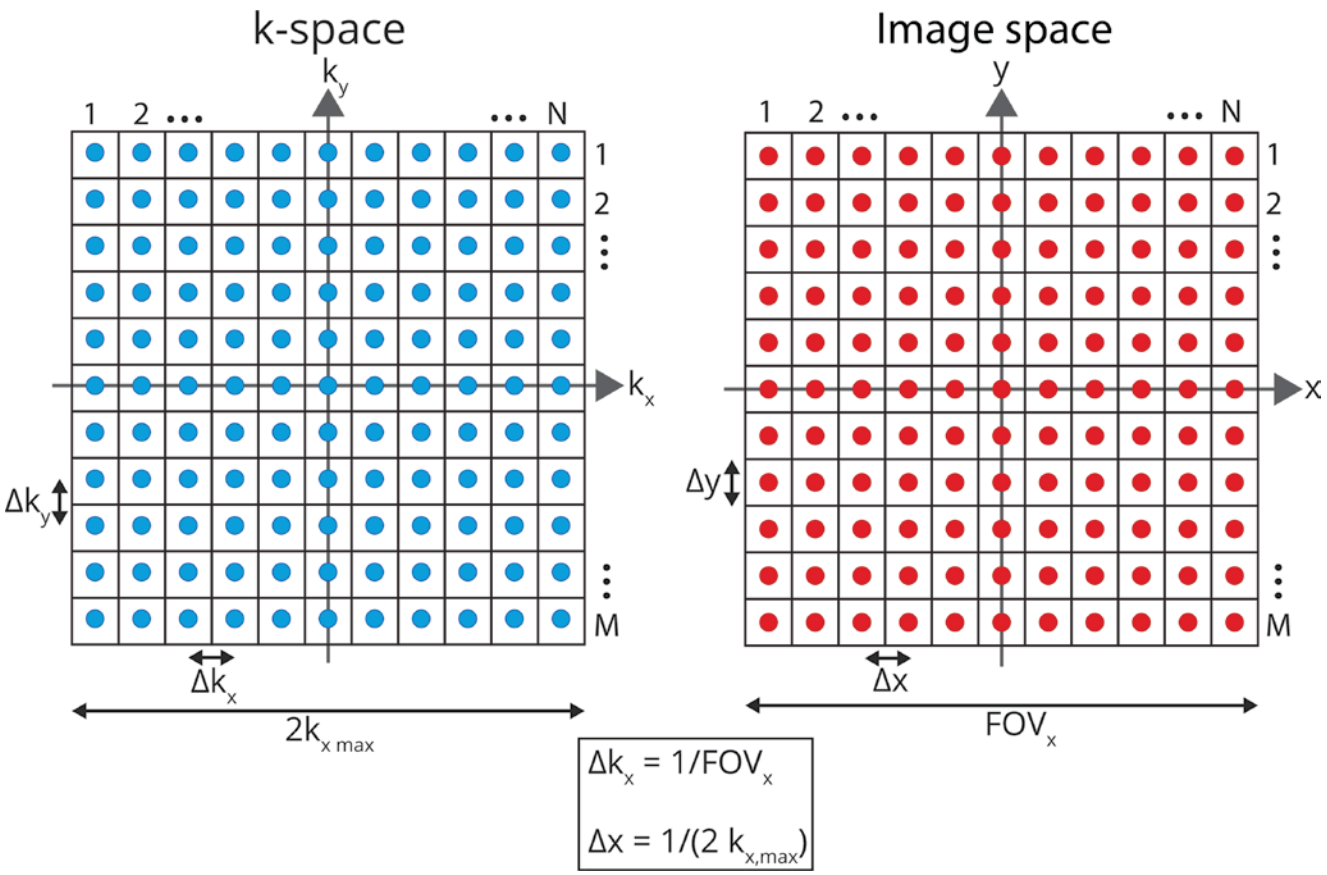

Fig. 2.6 Relationship between the sampling grids in k-space (*left*) and image space (*right*). MxN points are mapped from one domain to the other, and the relationship between the sample distance in k-space (Δkx and Δky) and the k-space coverage ($2*k_{x\,max}$ and $2*k_{y\,max}$) to the spatial resolution (Δx and Δy) and the covered field-of-view (FOV_x and FOV_y) is given in the equations above

Properties of k-Space

The Fourier transform is a commonly used tool in signal processing for signal filtering and conditioning. Therefore, an added advantage of the k-space formalism is that the impact that parameter choices in the sampling domain have on the resulting image are well characterized by the Fourier transform properties [3]. MR imaging involves the digitization of the acquired analog RF signal. Consequently, the fundamental laws of discrete data sampling and digital signal processing apply to MR data acquisition. The Nyquist-Shannon sampling theorem describes the k-space coverage required to reconstruct an image to the desired spatial resolution, as well the maximum separation between adjacent sampling points to ensure a field-of-view (FOV) without aliasing artifact. Figure 2.6 shows the relevant relations between the digital grids in k-space and in image space for the 2D case, which are explored in more detail here.

Spatial Resolution

The spatial resolution Δi in the resultant image is determined by the highest sampled spatial frequency ($k_{i\max}$):

$$\Delta i = 1/\left(2\,k_{i\max}\right) \tag{2.4}$$

where Δi is the spatial resolution in direction i. In other words, the voxel dimensions in the resultant image become smaller as the coverage of k-space increases further out from the center. This also implies that a higher resolution image requires more data samples, which usually results in longer scan time.

The information content of k-space regions with respect to their distance from the k-space origin are further illustrated in a cardiac in vivo scan reconstructed from different data samples in Fig. 2.7. The data points that represent the center of k space contain the low spatial frequencies, while the outer portions of k space contain the high spatial frequency information. In practical terms, this means that most of the image contrast is contained near the k-space center, while the outer portions define edges and are necessary to resolve small objects. Figure 2.7 shows that an image reconstructed from only the central 1 % of k-space will provide a general outline of the imaged object and some very low resolution contrast. The second column of Fig. 2.7 shows the image when the remaining 99 % of the outer portions of k-space are used in the reconstruction process. Now all the detailed structure can be identified but much of the underlying

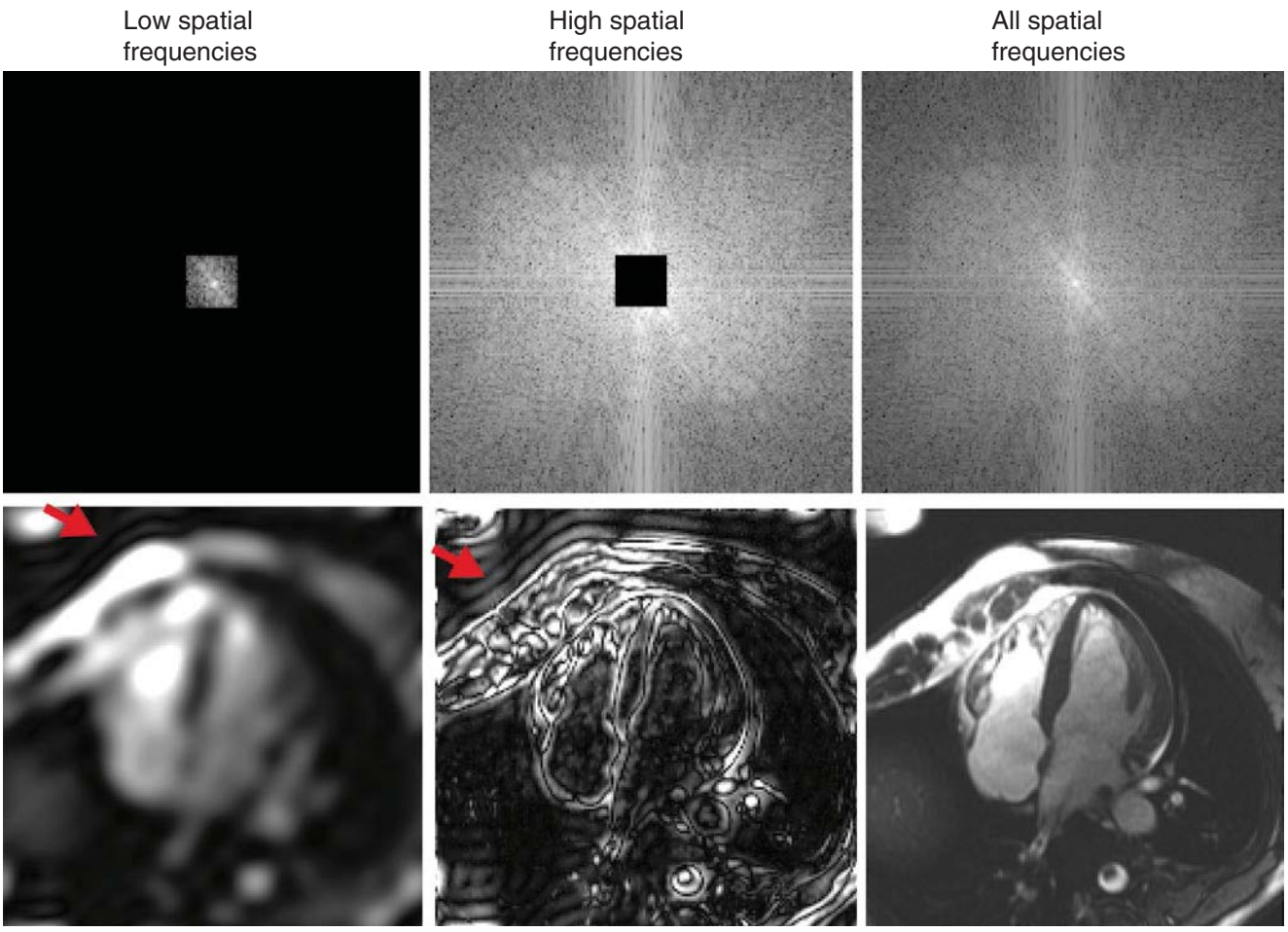

Fig. 2.7 Image contributions of low and high spatial frequencies in k-space. Low spatial frequencies are represented by the center of k-space, and define most of the image contrast, but lack edges or information on small objects. The periphery of k-space contains high spatial frequency information, which provides sharp edges in images. These images were reconstructed with 1 % of the central k-space data (*left column*) and 99 % of the higher spatial frequency data (*center column*). The *red arrows* point out ringing artifacts due to the k-space truncation, which are further discussed in other chapters

contrast has disappeared. These are basically low-pass and high-pass filtered images as a result of the omission of k-space regions.

This concept is frequently exploited in accelerated cardiovascular imaging, where high spatial frequency data are often undersampled at a higher degree than the low spatial frequency data in order to reduce total scan times without sacrificing significant information content.

Field-of-View

The separation between points in k-space, Δki, is proportional to the inverse of the FOV_i in image space:

$$\Delta k_i = \left(\frac{1}{FOV_i} \right) \tag{2.5}$$

where i represents the spatial dimensions x or y.

In other words, as the distance between sampled points in k space increases, the FOV of the resultant image decreases. A sufficient FOV is required in order to ensure ample coverage of the imaged object. Note that the k-space sampling grid and resultant FOV are independent along the two or three dimensions, meaning that the FOV and resolution can be set independently for each dimension.

Gradients and k-Space

As shown in Eq. 2.3, the actual k-space trajectory, i.e., the position in k-space at any time during data acquisition, is directly related to the product of the applied gradient field multiplied by the time since RF excitation, or more generally to the time integral of the gradient waveform. This is a powerful framework that allows us to control the gradients to steer our acquisition on a desired trajectory through k-space until all required data points are sampled. Note that from Eqs. 2.2

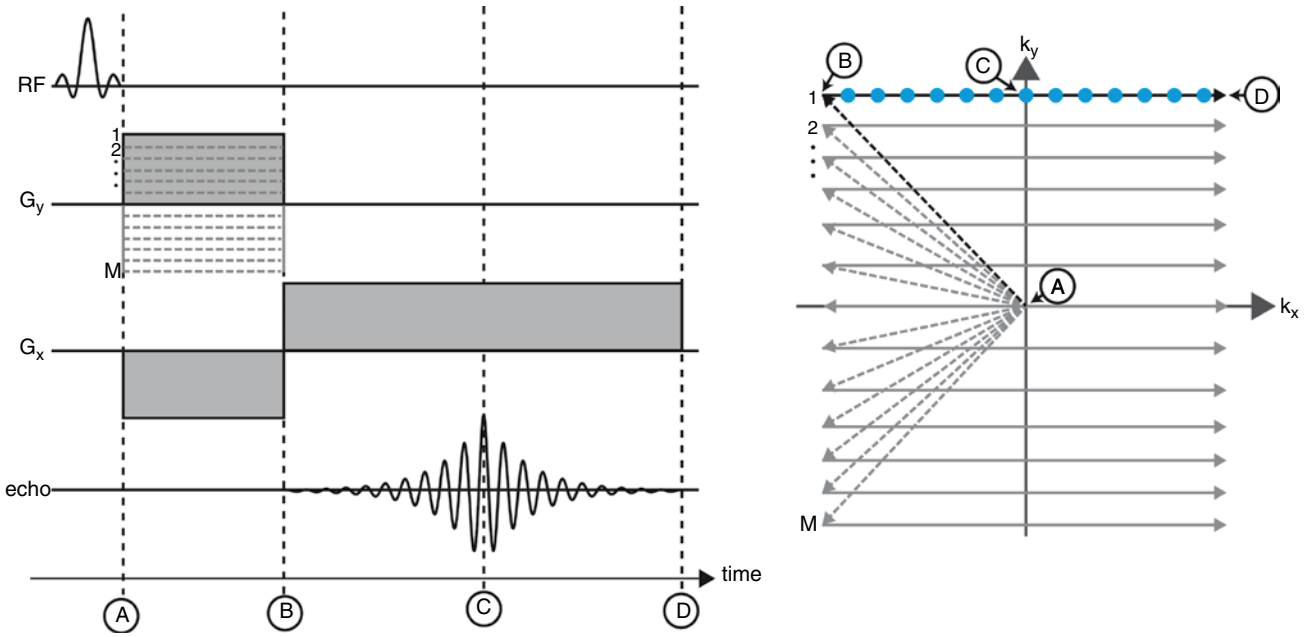

Fig. 2.8 Gradient waveforms are used to generate desired k-space trajectories, here shown for the spin warp acquisition of a simple 2D Cartesian trajectory using a gradient echo sequence. The k-space trajectory immediately after RF excitation always starts in the center of k-space (A). The use of a phase encoding gradient (G*y*) and frequency encoding gradient (G_X), also referred to as the readout gradient, establishes the path on the k-space grid as shown on the right. After the pre-winding gradients are played out at time B, the trajectory location is on the left edge of k-space and the acquisition is started. As the readout gradient is applied, data collection traverses through the center of k-space when the refocused echo occurs (time C). This point is also known as the echo time, or TE. Finally the acquisition of a single line is finished when the right edge of k-space is reached at time D. Data are sampled along lines parallel to the readout direction in equidistant spacing until all of k-space is covered

to 2.3, the k-space location of a given data point in the FID is located at $kx = G_X * t$, $ky = G_Y * t$, *and* $kz = G_Z * t$, where G_X, G_Y, and G_Z are the gradients in the *x*, *y*, and *z* directions.

Figure 2.8 illustrates the use of time varying gradients for a simple 2D gradient echo sequence with the commonly used spin-warp encoding [9] where data are sampled on a rectilinear Cartesian grid in lines parallel to the readout direction, *x*, at an acquisition speed of one line per excitation. A total of *M* lines is acquired by repeating the pulse sequence shown on the left. Each k-space line represents data sampled during a single echo formation, here generated by the gradient echo waveform labeled G_X. The combination of a pre-winding gradient between time points A and B, and the subsequent readout gradient between time points B and D, generates a gradient echo with its maximum amplitude at time point C. Therefore, this gradient is called the *readout gradient* and by convention it is usually labeled as the *x*-gradient, G_X. This acquisition is repeated *M* times with the only difference being variation of the amplitude of the G_Y gradient, which is played out as a short pulse simultaneously with the pre-winding lobe of G_X between time points A and B. Again by convention, this phase encoding gradient is usually labeled the y-gradient, G_Y, and phase encoding in 3D scanning is explored in a similar fashion along the *z* axis. Note that the use of G_X and G_Y is not meant to imply that the gradient coils on the x and y axis of the magnet are always used for readout and phase encoding, respectively; this is by convention only. In practice, the direction of the readout and phase-encoding gradients, while always orthogonal to each other, will vary in direction based on the image orientation, and for oblique imaging planes will require some combination of gradients in the x and y directions.

This combination of gradient waveforms results in the k-space sampling pattern displayed on the right of Fig. 2.8. By convention, the readout direction is usually displayed in the left-to-right direction on the k-space map. In this example, the first acquired k-space line is represented by the top row with blue dots for each data sample. At time point A, the spins have been excited and the trajectory starts at the origin of k-space. Between time points A and B, the G_X and G_Y gradients are both switched on with constant amplitude, thereby the k-space trajectory as determined by the product of gradient strength and time is steered towards the top left corner of the k-space map. Once that corner is reached at time point B, the phase encoding gradient is switched off and the frequency encoding gradient is inverted with identical amplitude. This leads to a trajectory parallel to the *kx* axis traveling across k-space from left to right, during which data are acquired. The system then returns to a steady state and this experiment is repeated *M* times while the amplitude of the phase encoding gradient is varied to step through equidistant parallel lines until the bottom row is sampled.

Consequently, the sampling intervals along the frequency encoding direction are determined by the sampling frequency of the analog-to-digital (AD) converter in the receiving chain and the amplitude of the readout gradient, while the sampling intervals along the phase encoding direction are determined by the increments in gradient amplitude.

As we have shown, we can think of gradients as 'driving' the acquisition through k-space, moving at a speed along each gradient direction directly related to the amplitude of the gradients. The trajectory design is ultimately limited by the maximum gradient amplitude (speed along a line) and by the maximum slew rate of the gradients (change of direction). Modern gradient systems used for medical imaging have undergone remarkable improvements over the past two decades to the point that their maximum performance is determined by safety limits to avoid peripheral nerve stimulation caused by rapidly switching magnetic fields. An important point to note is that *all* gradients in the pulse sequence influence the actual position in k-space, though k space *data* are only being recorded when the MRI scanner is actually acquiring data during the readout period.

Receiver Bandwidth

The sampling intervals, or spacing of samples in k-space, are controlled distinctively differently in the phase encoding direction and the frequency encoding (readout) direction. In the phase encoding direction, the increments in the area under the phase encode pulses directly determine the spacing of samples in the *ky* direction. In the readout direction, the sample spacing in time is ultimately dictated by the sampling frequency of the AD converter in the receiver chain. Once a desired spatial resolution and FOV is determined by the user, the number of data points in image space is established, which is identical to the number of k-space samples needed for each line. In the readout direction, not only the gradient strength but also the sampling rate can be adjusted to achieve the target sampling pattern in k-space. By increasing the amplitude G_x, we traverse faster through k-space. In order to maintain the proper number of samples and the desired distance in k-space, the sampling rate would also need to be increased and the duration of the acquisition window would be decreased. While this acquisition is identical in terms of k space sample points, there are several important implications in choosing the sampling frequency.

To avoid aliasing artifacts and decreased SNR performance due to external signal contributions, the receiver bandwidth has to be adjusted to the chosen sampling frequency, in practice by the operator. Depending on the system, this parameter is chosen either as a total bandwidth, e.g., 125 kHz, or in terms of Hz/pixel, the two being directly related as the product of Hz/pixel times the number of acquired data points (i.e., pixels across the FOV in the readout direction). Either way, the system automatically adjusts the gradient amplitude and sampling rate accordingly, effectively defining the time between samples (dwell time) while keeping the FOV constant. One of the first and most obvious consequences of increasing the receiver bandwidth is a decrease in the echo time (TE) because the increased gradient strength means that the echo forms faster, i.e., the readout crosses the center of k-space earlier. Shorter echo times are often desirable as they can shorten scan time in rapid imaging as well as decrease artifacts from intravoxel dephasing.

However, there are several other implications of changes in the receiver bandwidth, most importantly in SNR performance and in sensitivity to chemical shift artifacts. By increasing the receiver bandwidth, the readout gradient strength is increased, and thus the range of frequencies being imaged increases. Since noise contributions come equally from all frequency components, as the bandwidth increases, the noise content increases and SNR decreases. By increasing the bandwidth and allowing a wider frequency spectrum to measure the desired signal, more noise is added to the acquisition. The relationship between SNR and bandwidth is $SNR \propto 1/\sqrt{bandwidth}$; so, for example, increasing the bandwidth by a factor of four will decrease the image SNR by a factor of 2.

Additionally, the amount of spatial shifting in the image due to off-resonance (i.e., chemical shift) is inversely proportional to the receiver bandwidth. The common occurrence in clinical MRI of the chemical shift between fat and water illustrates this effect. When imaging at 1.5 T, the dominant fat peak has a frequency offset of about −220 Hz (3.5 ppm) as shown in Fig. 2.9. When imaging with a receiver bandwidth of ±31.25 kHz and a readout of 256 data points, the bandwidth is 2×31.25 kHz/256=244 Hz/pixel, and the corresponding chemical shift for fat is 1.1 pixels (256 Hz/244 Hz/pixel). In this example, fat will appear to be shifted by 1.1 pixels relative to water. Thus, when the receiver bandwidth is decreased, the SNR improves but the chemical shift worsens.

k-Space Sampling Trajectories

The sampling pattern described as spin warp imaging in section "Gradients and k-space" is by far the most commonly used k-space trajectory. In essence, k-space samples collected on a rectilinear checker board pattern with equidistant sampling points along each direction provide a framework where the computationally efficient Fast Fourier Transform (FFT) can be used for image reconstruction [10]. However, many alternative methods for traversing through k-space exist with certain potential advantages and tradeoffs. In the standard method of acquiring MR data, lines in k-space are "rastered" through, i.e., sampled one after another in a manner

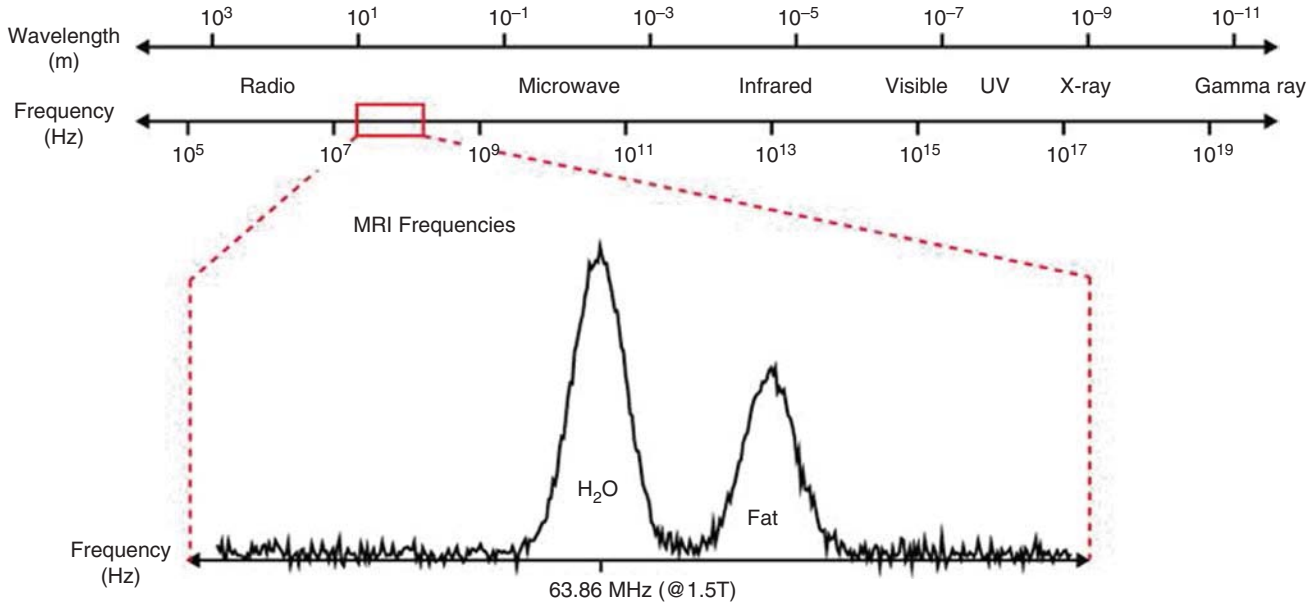

Fig. 2.9 Example of the MR imaging signal frequencies and their place in the entire electromagnetic spectrum. Here in this example, the spectrum is characterized by two peaks representing protons bound to water (on resonance) and fat (chemical shift of 3.5 ppm, corresponding to 220 Hz at 1.5 T)

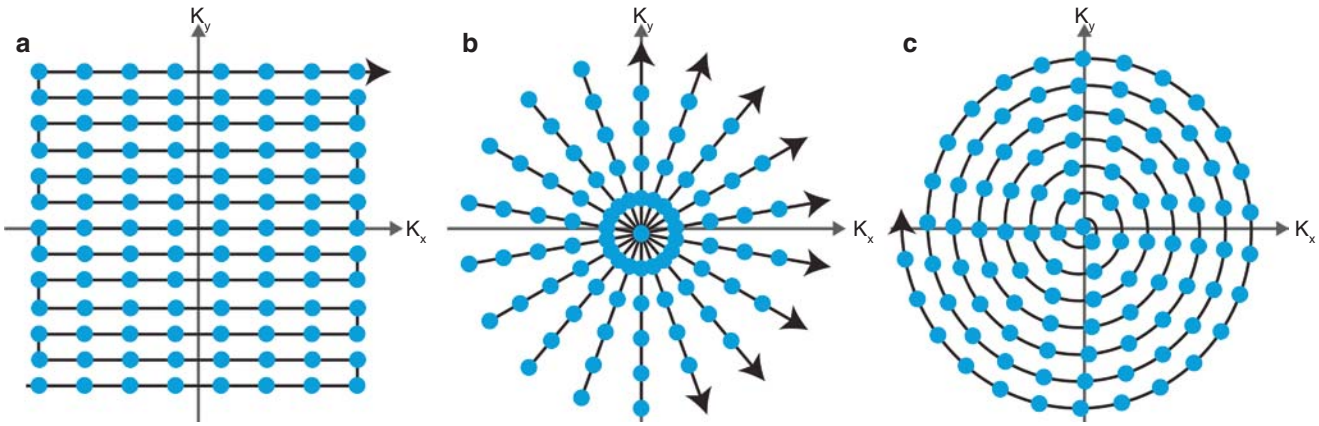

Fig. 2.10 Alternative k-space trajectories. (**a**) EPI, (**b**) radial, (**c**) spiral

reminiscent of cathode ray tube raster display systems, until k-space is fully sampled. Fully sampled, in this case, indicates that enough samples are acquired to reconstruct a full FOV image without aliasing artifact, while providing the desired spatial resolution. By deviating from this standard approach, k-space can be acquired at faster speeds with potential tradeoffs in image quality. The two main pathways for accelerated acquisitions with advanced sampling strategies are: (1) extending the readout duration, so that more k-space data can be sampled for each RF excitation, and (2) using sampling patterns to purposefully undersample k-space in a fashion that the resulting artifacts are acceptable and do not interfere with diagnosis.. There are numerous alternative trajectory approaches including radial, spiral, echo-planar imaging (EPI), PROPELLER, rosettes, cones, all in 2D and 3D, and many more. A complete review of these trajectories is beyond the scope of this chapter and instead, three methods frequently used in cardiovascular MRI will be briefly discussed: echo-planar imaging (EPI), radial, and spiral, which highlight the above two techniques for accelerating k-space acquisition and are shown in Fig. 2.10.

EPI

Echo-planar imaging is one of the most common forms of single-shot pulse sequences and was originally proposed in the very early days of MR imaging [11]. As the name implies,

single-shot imaging aims to acquire all of k-space with a single RF excitation and readout, as seen in Fig. 2.10a. The sequence works via a series of gradient or spin echoes, with 'blips' of the phase encode gradient in between to move between successive phase encode lines in k-space. The inherent limitation of EPI, and all single shot acquisitions, is that MRI signal decays rapidly due to various relaxation mechanisms, so the acquisition must be completed before extensive signal decay has occurred. This generally means that single-shot EPI images are of fairly low spatial resolution, but a single 2D image can be acquired extremely rapidly, in the range of 10–100 ms. EPI sequences can also lead to errors and artifacts due to phase inconsistencies such as chemical shift, susceptibility, and off-resonance effects, some of which can manifest inconsistently in the opposing readout directions caused by sampling during both positive and negative readout gradient lobes. These errors are more pronounced because spins are not necessarily being rephased on each readout line, causing some errors to accumulate and progressively worsen throughout the acquisition. The zigzag trajectory can also lead to cumulative trajectory errors that decrease image quality. Contrast in EPI sequences can be modified by using gradient-echo or spin-echo contrast mechanisms, or magnetization preparations such as saturation or inversion recovery. Multi-shot versions of EPI exist, where a smaller segment of k-space lines, i.e., less than required for the entire image, are acquired with each readout. This gives the user control over the trade-off between imaging speed and the resolution limitations/artifacts inherent with EPI.

Radial

Radial k-space trajectories, shown in Fig. 2.10b, are a non-Cartesian method, which means that points are not acquired on a rectilinear grid [12]. In the case of radial imaging, readout lines are designed as 'spokes' such that each pass through the center of k-space at different rotation angles. The inherent oversampling of the center of k-space where the spokes are naturally closer together leads to benefits for motion robustness and motion estimation, but also increases the total scan time when a fully sampled data set is desired. However, radial sequences are often accelerated by *undersampling*, which can be tolerable in high contrast imaging such as cardiac applications of balanced SSFP. Unlike fold-over artifact in Cartesian imaging, radial undersampling produces 'streaking' artifact, which can be minimal if moderate undersampling factors are chosen. The tradeoffs with radial acquisitions are twofold: the first is that reconstructions take longer because data must be gridded back onto a Cartesian k-space before a Fourier transform can be applied, and the second tradeoff is the increased sensitivity to trajectory errors that have to be carefully corrected for. Since the readout direction changes with each echo, the center of k-space might be missed slightly due to minimal gradient delays or uncompensated eddy currents. These trajectory deviations add phase errors and blurring to the reconstructed image, though techniques can be used to measure these gradient offsets and compensate for them to mostly eliminate the errors.

Spiral

Spiral acquisitions combine both of the acceleration techniques described above: longer readouts to achieve higher k-space coverage with a single RF excitation, and a non-Cartesian trajectory so that aliasing is more benign [13]. There are various implementations of spiral trajectories but most spiral out from the center of k-space as shown in Fig. 2.10c. Single-shot versions of spiral exist and are used as an alternative to EPI, however multiple interleaved versions of spiral are also common. With multiple interleaves, each spiral starts in the center of k-space, while stepping through angles for each new interleave. Like EPI, spiral imaging is vulnerable to off-resonance effects due to the long TR, and like radial acquisitions it requires a computationally more demanding gridded reconstruction and can suffer from trajectory errors caused by eddy currents and gradient delays that must be accounted for.

References

1. Bernstein MA, King KF, Zhou ZJ. Handbook of MRI pulse sequences. Amsterdam: Academic; 2004.
2. Liang Z-P, Lauterbur P C, and IEEE Engineering in Medicine and Biology Society. Principles of magnetic resonance imaging: a signal processing perspective. Bellingham/New York: SPIE Optical Engineering Press/IEEE Press, 2000.
3. Bracewell RN. The fourier transform and its applications. New York: McGraw-Hill; 2000.
4. Hinshaw WS. Spin mapping – application of moving gradients to Nmr. Phys Lett A. 1974;A 48(2):87–8.
5. Mezrich R. A perspective on K-space. Radiology. 1995;195:297–315.
6. Likes R S. Moving gradient zeugmatography, US patent 430734, USA, 1981.
7. Ljunggren S. A simple graphical representation of Fourier-based imaging methods. J Magn Reson. 1983;54:338–43.
8. Twieg DB. The k-trajectory formulation of the NMR imaging process with applications in analysis and synthesis of imaging methods. Med Phys. 1983;10:610–21.
9. Edelstein WA, Hutchison JM, Johnson G, Redpath T. Spin warp NMR imaging and applications to human whole-body imaging. Phys Med Biol. 1980;25(4):751–6.
10. Brigham EO, Brigham EO. The fast Fourier transform and its applications. Englewood Cliffs: Prentice Hall; 1988.
11. Mansfield P. Multi-planar image formation using NMR spin echoes. J Phys C Solid State Phys. 1977;10:L55.
12. Lai CM, Lauterbur PC. True three-dimensional image reconstruction by nuclear magnetic resonance zeugmatography. Phys Med Biol. 1981;26(5):851–6.
13. Meyer CH, Hu BS, Nishimura DG, Macovski A. Fast spiral coronary artery imaging. Magn Reson Med. 1992;28:202–13.